ChemPlusChem

Research Article
doi.org/10.1002/cplu.202300421

Chemistry Europe
European Chemical Societies Publishing

www.chempluschem.org

Special Collection

Insights on the Anion Effect in N-heterocyclic Carbene Based Dinuclear Gold(I) Catalysts

Filippo Campagnolo[+],[a] Matteo Bevilacqua[+],[b] Marco Baron,*[b] Cristina Tubaro,[b] Andrea Biffis,[b] and Daniele Zuccaccia*[a]

Dinuclear bisNHC (bis(N-heterocyclic carbene)) gold(I) complexes **3a** and **4a** of general formula [Au_2Br_2(bisNHC)] were tested as catalysts in the cycloisomerization of *N*-(prop-2-yn-1-yl)benzamide and in the hydromethoxylation of 3-hexyne in the presence of silver(I) activators bearing different counteranions. The catalytic performance of mononuclear NHC complexes (**1a**, **2a**) in the same reactions was also studied. The results highlighted the fundamental role of both NHC ligand and counterion in the catalytic cycles and activation process: dinuclear catalysts exhibit higher initial activity even under milder conditions but suffer in terms of stability with respect to mono NHCs. Furthermore, a new dinuclear bisNHC gold(I) complex **4b** of general formula [Au_2(OTs)$_2$(bisNHC)] (OTs = *p*-toluenesulfonate) was successfully synthesized and characterized by means of NMR and ESI-MS analyses.

Introduction

Gold chemistry is acknowledged for its importance due to the metal's unique reactivity, which is relevant for synthetic applications in the pharmaceutical industry.[1] Given the soft character of the metal, gold(I) complexes activate unsaturated compounds toward nucleophilic attacks.[2–4] In recent years, linear gold(I) complexes (L–Au–X) featuring *N*-heterocyclic carbene (NHC) as ligands were under the spotlight due to high reactivity matched by improved stability when compared to gold(I) phosphine complexes.[5,6] Despite that, homogeneous gold(I) complex catalyzed reactions are still limited by the required high catalyst loadings and the extensive use of volatile organic solvents (VOS).[7,8] In our previous publications, we described the pivotal role of the counterion (X^-, Figure 1), as it is not only merely a spectator but is instead involved in the reaction mechanism.[9] As the catalyst enters in the pre-equilibrium step, the counterion moves from the inner-sphere ion pair (ISIP) to the outer-sphere ion pair (OSIP). At this point, the counterion engages in the critical steps of the reaction mechanism, acting both as a templating agent during the nucleophilic attack and as a proton shuttle in the proto-deauration step.[1,9–11]

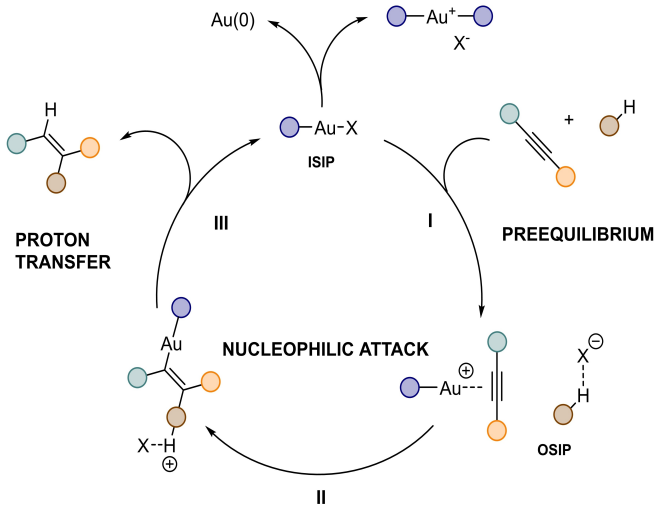

Figure 1. Generally accepted reaction mechanism for gold(I) complex catalyzed reactions involving alkynes. The critical reaction steps have been numbered (I–III), and in the pre-equilibrium step, the shift of the counterion from the inner-sphere (ISIP) to the outer-sphere (OSIP) ion pair has been highlighted.

Consequently, the counterion must be carefully chosen, considering in first instance its coordinative properties, since strongly coordinating anions will not detach from the catalyst preventing its activation, while non-coordinating anions will not be able to interact with the activated substrate.[12] Catalysts bearing trifluoromethanesulfonate (OTf^-) and p-toluenesulfonate (OTs^-) generally displayed the highest TOFs when the rate-determining step (RDS) is the nucleophilic attack. Conversely, non-coordinating anions like hexafluorophosphate (PF_6^-) per-

[a] F. Campagnolo,[+] Prof. Dr. D. Zuccaccia
Dipartimento di Scienze Agroalimentari, Ambientali e Animali
Università di Udine
Via Cotonificio 108
33100 Udine (Italy).
E-mail: daniele.zuccaccia@uniud.it

[b] M. Bevilacqua,[+] Dr. M. Baron, Prof. Dr. C. Tubaro, Prof. Dr. A. Biffis
Dipartimento di Scienze Chimiche
Università degli Studi di Padova
Via Marzolo 1
35131 Padova (Italy)
E-mail: marco.baron@unipd.it

[+] F.C. and M.B. contributed equally to this work.

Supporting information for this article is available on the WWW under https://doi.org/10.1002/cplu.202300421

Special Collection Part of a Special Collection on Gold Chemistry

formed best when the proton-shuttling is the RDS. In summary, coordinating counterions do not ionize entirely, reducing the amount of active complex in the catalytic cycle (Figures 1 and 2, I), but they are required if the nucleophilic attack is the RDS: the basic properties of the anion become essential to drive nucleophile activation. Since basic and coordinative properties are closely tied, OTs^- proved to be the more suitable anion (Figures 1 and 2, II). On the contrary, when the RDS is the proto-deauration step, the basic properties of the anion will hinder the proton-shuttling, slowing down the reaction due to the formation of stable HX, and hence non-coordinating anions such as PF_6^- or BF_4^- become more efficient (Figures 1 and 2, III).

The solvent also plays a vital role, as low-polarity media proved to be more effective in catalysis, whereas increasing the polarity of the medium decreased the reactivity,[7,13] even if some of us have shown that green polar solvents can be used in gold catalysis if they have the right chemical functionality to promote the various steps of the catalytic cycle.[8] In apolar solvents, we assumed that the ion-pairing between catalyst and anion also plays a crucial role in terms of reactivity, dictating the actual amount of the catalyst in the active form, which involves an intimate ion-pair.

Moreover, when studying the reactivity of gold(I) complexes in catalysis, attention should be paid to those systems being affected by deactivation. Ligand-induced deactivation is significant with gold(I) phosphine catalytic systems,[14] however, its contribution is limited when complexes bearing NHC ligands are involved, and it is negligible if these feature sterically demanding wingtips. Cationic gold disproportionation and deactivation can be modulated by the substrate, nucleophile and silver additives.[15,16]

Within this context, dinuclear NHC gold(I) complexes are a recent novelty in the field of homogeneous gold catalysis.[17–21] Dinuclear gold species have recently gathered attention in connection with the study of digold catalysis, i.e. the formation of digold species and their involvement in a catalytic reaction.[22–25] In many cases, digold compounds have been identified as resting forms of catalysts,[26] but in some cases a beneficial effect in the use of digold catalysts has been reported, as demonstrated by Nolan and coworkers for the hydroalkoxylation of alkynes with aromatic alcohols, such as phenol and its derivatives.[27] To the best of our knowledge, digold systems have been tested to a small extent in terms of rationalization of ion-pairing, activation process and deactivation effects. In this work we aim at analyzing the above mentioned effects when dinuclear gold(I) complexes of general formula $[AuX_2(bisNHC)]$ (X = anionic ligand) are employed as catalysts. For this purpose, we selected two different benchmark organic transformations, namely the cycloisomerization of *N*-(prop-2-yn-1-yl)benzamide, and the hydromethoxylation of 3-hexyne.

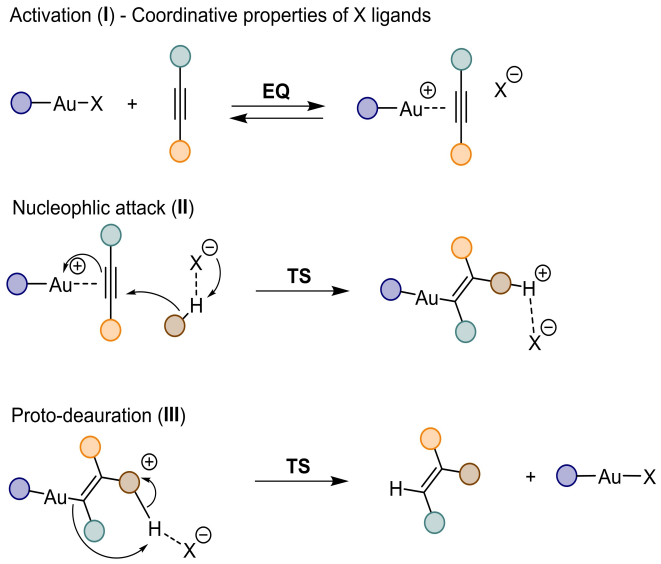

Figure 2. Possible RDS in the gold(I) catalyzed hydrofunctionalization of alkynes.

Results and Discussion

Synthesis of the gold(I) complexes

The gold(I) complexes **1a**–**4a** have been synthesized from the respective imidazolium salts by following reported procedures (Figure 3).[19,21,28] In the frame of the catalytic studies, the complexes were activated *in situ* with trifluoromethanesulfonate (OTf^-), *p*-toluenesulfonate (OTs^-), and hexafluorophosphate (PF_6^-) via metathesis with silver salts.

The derivative of complex **4a**, bearing OTs^- (**4b**), was isolated and characterized by means of NMR spectroscopy and ESI-MS spectrometry (Figure 4).

The ^1H NMR spectrum of complex **4b** shows a slightly shifted set of signals for the bisNHC ligand compared to **4a**. Moreover, the presence of the OTs^- anion is confirmed by presence of the expected *p*-tolyl group signals. In the ^{13}C NMR spectrum of **4b** the carbene carbon signal in $CDCl_3$ is upfield shifted to 162.4 ppm with respect to the pristine bromido complex **4a** (176.2 ppm), in agreement with what was observed in the case of the mononuclear complex IPrAuBr. The ^{13}C NMR carbene carbon chemical shifts for IPrAuOTs (**1b**) and IPrAuBr

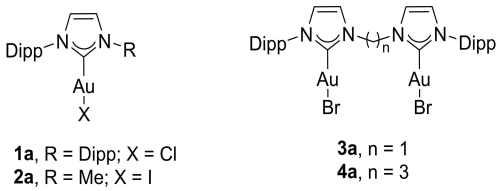

Figure 3. Gold(I) complexes used in this work.

Figure 4. Synthesis of complex **4b**.

are in fact 164.6 and 179.0 ppm ($CDCl_3$).[28,29] In the ESI-MS spectrum of **4b**, the base peak is represented by the signal of the $[Au_2(bisNHC)OTs]^+$ species at 1061.28 *m/z*. Furthermore, there are no signals of Br^- derivatives, indicating that the bromide abstraction occurred quantitatively. Even though complex **4b** was not used directly in the catalytic experiments, it was used in the model NMR experiments performed to gain insights about the reaction mechanism (*vide infra*).

Catalytic studies on the cycloisomerization of N-(prop-2-yn-1-yl)benzamide

Complexes **2a**–**4a** were tested in the cycloisomerization of N-(prop-2-yn-1-yl)benzamide (Figure 5), and the reaction profile was tracked through ^{1}H-NMR spectroscopy. The halide complexes were activated *in situ* using silver salts bearing OTs^-, OTf^-, and PF_6^- groups. We employed the initial rates method to compare the performances of catalysts **2a**–**4a** (Figure 5).

The data confirm the trend observed in our previous publications: low-polarity solvents return the best results, with chloroform being more suitable as a solvent than nitromethane. When looking at the reactivity of complexes **2a**–**4a** in the different media but with the same counterion we observe a clear trend, dinuclear catalysts reacting slightly faster. The anion effect also matched earlier results with non-coordinating anions like PF_6^- displaying the best overall performances in the cycloisomerization reaction. Indeed, the basic properties of anions such as OTs^- and OTf^- inhibit proton shuttling, which is this reaction rate-determining step (RDS).

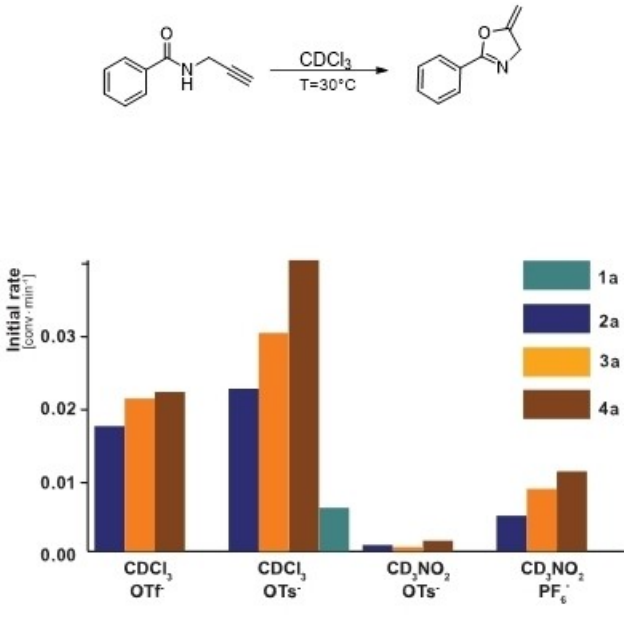

Figure 5. Cycloisomerization of N-(prop-2-yn-1-yl)benzamide. Reaction conditions: 1 mol% mononuclear complex or 0.5 mol% dinuclear complex, activator 1 mol%, substrate concentration 0.5 M (top). Comparisons of initial rates in the N-(prop-2-yn-1-yl)benzamide cycloisomerization reaction for catalysts **1a**-**4a** under different reaction conditions (bottom). Complex **1a** was used as a benchmark.

Complex **4a**, which features a propylene linker, almost doubles the reactivity of complex **2a** and the difference is even more marked with respect to reference complex **1a** (Table 1, Figure 5).

The different reactivity between mononuclear and dinuclear gold(I) complexes could be explained in terms of anion dissociation energy during the pre-equilibrium step (Figure 2**, I**). Indeed, it must be borne in mind that in dinuclear complexes aurophilic interactions between the two gold(I) centers can be established not only in the solid state but also in solution, as we have demonstrated by means of cyclic voltammetry experiments.[17] If present, this weak interaction can affect the physical-chemical properties of the considered gold(I) complexes as well as their reactivity and catalytic performances.[19,30–32] We have also recently demonstrated that the establishment of aurophilic interactions might facilitate the exchange of the anionic ligand (X^-) with neutral ligands (L), *i.e.* the ISIP to OSIP conversion.[18] Among the different possible linkers between the two NHC donors of the bisNHC ligand, the propylene one owns the right length and flexibility to maximize aurophilicity in the molecule. Thus, not surprisingly, complex **4a**, bearing the most flexible bridge is the one most amenable to present such aurophilic interactions.[33]

In order to get some experimental evidence of that, we performed ^{1}H NMR experiments in $CDCl_3$ on the substrate effect on the ISIP/OSIP chemical equilibrium for the preformed dinuclear catalyst **4b**. We used 2,3-dimethyl-2-butene as model substrate (Figure S20). At room temperature and without the coordinating substrate, the *p*-toluenesulfonate peaks are broadened due to the exchange equilibrium occurring with water traces in the deuterated solvent, the aromatic signals of the anion falling respectively at 7.17 and 7.77 ppm. After adding 2,3-dimethyl-2-butene, two doublets appeared up-field at 7.34 and 7.80 ppm, an increase consistent with a shift in the equilibrium between the ISIP and OSIP ratio of the anion due to substrate competition. It was possible to estimate from signals integration that the percentage of OSIP was already around 20% when 20 equivalents of 2,3-dimethyl-2-butene were added to a solution of **4b** in $CDCl_3$.

The behavior of **4b** in this model experiment is quite different compared to **1b**. In fact, previous literature findings concerning **1b**,[29] showed that in aprotic solvents and with an excess of 3-hexyne as substrate, the equilibrium between

Table 1. The catalytic results of catalyst **1a**–**4a** in the cycloisomerization of N-(prop-2-yn-1-yl)benzamide, where $CDCl_3$ was used as a solvent and AgOTs was employed as the activator.[a] The initial rate is expressed as the reagent relative conversion over minutes.

Catalyst	Initial rate/ conv·min^{-1}	TOF^{50}/ h^{-1}	t/h	Conversion/ %
1a	0.006	20	24.0	95
2a	0.025	136	3.0	98
3a	0.030	350	1.6	97
4a	0.040	460	1.2	98

[a] See the Experimental Section for details.

[IPr–Au-OTs] (ISIP) and [IPr–Au-(3-hexyne)]$^+$OTs$^-$ (OSIP) was completely shifted toward ISIP. Since a weak frequency shift and peak broadening were observed after the 3-hexyne addition, it was inferred that anion and substrate were involved in a dynamic equilibrium with the [IPr–Au]$^+$ fragment, proving that OSIP is thermodynamically less favored than ISIP, but still kinetically accessible. Moreover, the addition of methanol further affected the equilibria releasing the free uncoordinated OTs$^-$ in solution.[29] The formation of the OSIP is thus favored in dinuclear complexes compared to mononuclear ones and this is reflected in the catalytic performances. When considering TOF^{50} we notice the same reactivity, with complex **4a** (Table 1, 460 h^{-1}) that remains more active with respect to complexes **2a** (Table 1, 136 h^{-1}) and **3a** (Table 1, 350 h^{-1}).

Catalytic studies on the hydromethoxylation of 3-hexyne

Complexes **1a**–**4a** were also tested in the hydromethoxylation of 3-hexyne using AgOTs as activator (Figure 6, Table 2).

Catalysts **2a** and **4a** reached 67% conversion after 70 minutes, whereas **3a** hit 37%; all catalysts achieved completion in 18 hours.

The new trend sharply contrasts with previous findings in the cycloisomerization reaction, especially after considering the four-fold rate increase of catalyst **1a** compared to **2a**–**4a**, based on TOF^{50} values.

The reason could be ascribed either to a reaction RDS change, from the proto-deauration step in the cycloisomerization to the nucleophile attack in the hydroalkoxylation reaction, or to a pre-equilibrium/deactivation process. Since this matter required further investigation, a series of NMR experiments were conducted to identify possible relevant intermediates. These experiments were designed to mimic the chemical environment at the pre-equilibrium phase, while preventing the hydromethoxylation reaction from occurring. For this reason, we used the same reaction conditions of the catalytic tests reported in Table 2 in terms of quantities of substances, but we replaced 3-hexyne with 2,3-dimethyl-2-butene. Under these pseudo-catalytic conditions, we recorded the ^{1}H NMR spectra before and after the addition of AgOTs. The test carried out with **4a** resulted in two unique sets of catalyst-related signals, each accounting for the same abundance. In order to understand the nature of these two species, we employed the ^{1}H-PGSE NMR technique, which can be used to determine molecules' diffusion coefficients and calculate the average hydrodynamic volumes.[34,35] From the PGSE experiments, the hydrodynamic volume of complex **4a** before adding AgOTs was calculated to be 1677 Å^3. After adding the silver salt, the two sets of signals from different catalyst-derived species appeared, and each species volume was calculated to be 1912 Å^3 and 4564 Å^3. The species with the smaller hydrodynamic volume can be interpreted as an average of the pseudo-catalytic competent species. The bigger species has a hydrodynamic more than doubled compared to the starting complex **4a**, and this can be rationalized with the formation of a metallacyclic dimer [Au$_2$(bisNHC)$_2$]$^{2+}$ that is inactive in the catalysis. This type of reactivity has been already described in the literature.[36,37]

While deactivation was not observed in the case of **1a**, as the steric bulkiness results in a lower tendency to produce the [Au(NHC)$_2$]$^+$ species, it appears that this deactivation pathway is significant with less sterically hindered catalysts like **2a**–**4a**.

Adding the results obtained from the hydroalkoxylation of 3-hexyne to the ones discussed above from the cycloisomerization of *N*-(prop-2-yn-1-yl)benzamide, it becomes clear that the methanol used as a reactant in the hydroalkoxylation increases the polarity of the media, affecting the amount of active **1a** catalyst. Hence, the increased reactivity of complexes **3a**–**4a** in the cycloisomerization could be ascribed to the aforementioned easier dissociation of the anion in these complexes, which is also evidently linked to the deactivation processes involving the formation of homoleptic gold(I) NHC cationic complexes boosted by the polar and protic media.

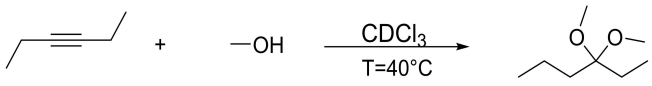

Figure 6. Hydromethoxylation of 3-hexyne. Reaction conditions: 3-hexyne (0.6 mmol), MeOH (1.2 mmol), and $CDCl_3$ (0.35 mL), 1 mol% mononuclear complex or 0.5 mol% dinuclear complex, activator (AgOTs) 1 mol% with respect to the alkyne.

Table 2. The catalytic results of catalysts **1a**–**4a** in the hydroalkoxylation of 3-hexyne, where $CDCl_3$ was used as a solvent and AgOTs was employed as activator.[a]

Catalyst	TOF^{50}/h^{-1}	t/h	Conversion/%
1a	250	0.3	99
2a	60	18	97
3a	40	18	97
4a	60	18	97

[a] See the Experimental Section for details.

Conclusions

The catalytic activity of two monocuclear NHC gold(I) complexes **1a** and **2a** and of two dinuclear bisNHC gold(I) complexes **3a** and **4a** in the cycloisomerization of *N*-(prop-2-yn-1-yl)benzamide and in the hydromethoxylation of 3-hexyne was investigated. Moreover, the synthesis of a new dinuclear bisNHC gold(I) complex **4b**, bearing *p*-toluenesulfonate (OTs$^-$) anions, was reported. The catalytic activity of the NHC-gold(I) complexes reported herein strongly depends on the nature of the counterion due to the already acknowledged role played by the latter in the reaction mechanism. However, the anion effect does not comprehensively explain the reactivity. As we assumed in our previous publication, the formation of intimate OSIP ion pairs, between the substrate coordinated cationic complex and the anion, regulates the actual concentration of the catalyst active form in solution. In this connection, the anion dissociation process, a critical step in catalyst activation process, contributes significantly in low-polarity media, such as those

under which the cycloisomerization of *N*-(prop-2-yn-1-yl)benzamide is carried out. Catalysts **2a**–**4a** have a lower activation energy barrier when compared to more sterically demanding catalysts like **1a**. On the contrary, less sterically demanding NHCs easily undergo deactivation forming homoleptic gold(I) NHC complexes in polar environments, such as those under which the hydromethoxylation of 3-hexyne is carried out. When dealing with dinuclear gold(I) catalysts there is an additional factor to take in consideration, in fact, the interaction between the two gold(I) centers can affect the formation of the active catalytic species. A stronger aurophilic interaction facilitates the anion dissociation process. This makes the dinuclear complexes **3a** and **4a**, more active than the mononuclear complexes **1a** and **2a** in the cycloisomerization of *N*-(prop-2-yn-1-yl)benzamide. Complex **4a**, that has the molecular structure in which aurophilicity is favored for the presence of the flexible propylene bridging group is the most active catalyst in this reaction. Differently, in the hydromethoxylation of 3-hexyne, the dinuclear complexes are partially deactivated due to the formation of the homoleptic cationic complexes $[Au_2(bisNHC)_2]^{2+}$.

Hence, fine tuning of the anion-coordinative properties is crucial when dealing with dinuclear catalysts **3a**–**4a**, because these complexes do easily release the counterion in the pre-equilibrium step, a feature that enhances the catalytic performances in apolar media while driving deactivation in polar media.

Experimental Section

All manipulations, unless otherwise noted, were carried out under argon atmosphere, using standard Schlenk techniques. All the reactants and the solvents were obtained from commercial suppliers and used as received. Gold complexes **1a**,[28] **2a**,[21] **3a**[19] and **4a**[19] were prepared by following literature procedures.

^{1}H and ^{13}C NMR spectra were recorded at 298 K on a Bruker Avance 300 MHz (7.05 T) operating at 300.1 and 75.5 MHz, respectively or with a Bruker Avance III HD 400 MHz spectrometer equipped with a broadband 5 mm probe (^{1}H/BBF iProbe) with a z-axis gradient (50G/cm). Chemical shifts are reported in parts per million and calibrated to the solvent residue. ^{1}H NMR signals are labeled as s = singlet, d = doublet, t = triplet, q = quartet, sept = septet and m = multiplet. ESI mass spectra were recorded on a Finnigan Thermo LCQ-Duo ESI mass spectrometer operating in positive ion mode; sample solutions were prepared by dissolving the compounds in methanol and were directly infused into the ESI source by a syringe pump at 8 μL/min flow rate.

Synthesis of 4b – Complex **4a** (19.2 mmol, 20.2 mg) was dissolved in 2 mL of dry DCM. The obtained orange solution was protected from light using an aluminum foil and, under stirring, solid AgOTs (38.0 mmol, 10.6 mg) was added. The mixture was left under stirring for 1 h. Whist after a few minutes it is possible to notice the formation of a black-grey precipitate, the solution color remains unchanged. AgBr precipitate was filtered with a PTFE (0.2 μm) filter and the solution was concentrated under reduced pressure to a volume of ca. 0.2 mL. Subsequently, 5 mL of *n*-hexane were added, affording a brown/orange precipitate. The solid was decanted and washed with *n*-hexane (5 mL x 2). The obtained product was dried under reduced pressure to obtain a brown solid. Yield 83% (15.9 mmol; 19.6 mg). ^{1}H-NMR (300 MHz, $CDCl_3$): δ 7.75 (m, br, 4H, CH^{OTs} aromatic + 2H CH imidazole), 7.50 (t, J = 7.80 Hz, 2H, CH^{Dipp} aromatic), 7.25 (m, 4H, CH^{Dipp} aromatic), 7.18 (d, J = 7.80 Hz, 4H, CH^{OTs} aromatic), 7.00 (d, J = 1.77 Hz, 2H CH imidazole), 4.52 (t, J = 7.75 Hz, 4H, NCH_2), 2.98 (br, 2H, $-CH_2-$), 2.38 (m, 4H, CH^{Dipp} + 6H CH_3^{OTs}), 1.26 (d, J = 6.80 Hz, 12H, CH_3^{Dipp}), 1.14 (d, J = 6.80 Hz, 12H, CH_3^{Dipp}). ^{13}C NMR (75.50 MHz, $CDCl_3$): δ = 161.6 (NCN), 146.6 (C aromatic), 134.9 (OTs), 134.7 (OTs), 131.6 (OTs), 129.9 (CH aromatic), 127.2 (OTs), 125.2 (CH imidazole), 125.0 (CH aromatic), 123.7 (CH imidazole), 49.8 ($CH_2CH_2CH_2$), 34.5 ($CH_2CH_2CH_2$), 29.4 (CH), 25.4 (CH_3), 22.4 (CH_3) ppm. ESI-MS (*m/z*): $C_{40}H_{51}Au_2N_4O_3S$, $[M\text{-}OTs]^+$, calc. 1061.28, obs. 1061.28.

Catalytic tests on the cycloisomerization of *N*-(2-Propyn-1-yl)benzamide. A 4 mL vial was charged with the gold(I) complex and *N*-(2-propyn-1-yl)benzamide (0.25 mmol, 40 mg). The amount of gold(I) complex was calculated relative to the number of metal centers in the catalysts. Hence, the catalyst loading for mononuclear complexes is 1% mol ($2.5\cdot10^{-3}$ mmol), and 0.5% mol ($1.3\cdot10^{-3}$ mmol) for dinuclear complexes. The compounds were dissolved in 0.5 mL of deuterated solvent, and transferred to a 5 mm NMR tube previously charged with the silver(I) salt ($2.5\cdot10^{-3}$ mmol). A kinetic experiment was carried out using the zg2d pulse sequence on ^{1}H nucleus at 30 °C to collect the reaction profile.

Catalytic tests on the hydromethoxylation of 3-hexyne. A typical catalytic experiment was performed in a Schlenk tube equipped with a magnetic stirring bar. Initially, the gold(I) complex and the silver(I) salt co-catalyst were placed under an inert atmosphere. Then, methanol (1.2 mmol, 48 μL), 3-hexyne (0.6 mmol, 68 μL) and $CDCl_3$ (0.35 mL) were mixed and injected into the Schlenk tube. Subsequently, the reaction vessel was placed in an oil bath warmed at 40 °C and the mixture was stirred for the selected reaction time. The mixtures were analyzed by ^{1}H NMR spectroscopy after 70 minutes and 18 hours under warming. Alkyne conversion was calculated by ^{1}H NMR.

Diffusion NMR. ^{1}H PGSE NMR measurements were performed by using the double stimulated echo version with longitudinal eddy current delay on a Bruker Avance III HD 400 spectrometer equipped with a Iprobe (400 MHz for ^{1}H) with a z gradient coil. The dependence of the resonance intensity (I) on a constant waiting time and on a varied gradient strength G is described by the following equation 1:

$$\ln\frac{I}{I_0} = -(\gamma\delta)^2 D_t\left(\Delta - \frac{\delta}{3}\right)G^2 \quad (1)$$

where I is the intensity of the observed spin echo, I_0 the intensity of the spin echo in the absence of gradient, D_t the self-diffusion coefficient, Δ the delay between the midpoints of the gradients, δ the length of the gradient pulse, and γ the magnetogyric ratio. The shape of the gradients was rectangular, their length δ was 4–5 ms, and their strength G was varied during the experiments. The semilogarithmic plots of $\ln(I/I_0)$ versus G^2 were fitted by using a standard linear regression algorithm, and a correlation factor better than 0.99 was always obtained. The self-diffusion coefficient D_t, which is directly proportional to the slope m of the regression line obtained by plotting $\ln(I/I_0)$ versus G^2, was estimated by evaluating the proportionality constant for a sample of HDO (5%) in D_2O (known diffusion coefficients in the range 274–318 K)[38] under the exact same conditions as the sample of interest. The solvent (or 2,3-dimethyl-2-butene) was taken as internal standard. The Dt data were treated as described in the literature to derive the hydrodynamic dimensions.[39,40]

Acknowledgements

Prof. Paolo Sgarbossa (University of Padova) is kindly acknowledged for the ESI-MS measurements.

Conflict of Interests

The authors declare no conflict of interest.

Data Availability Statement

The data that support the findings of this study are available from the corresponding author upon reasonable request.

Keywords: carbenes · gold · dinuclear catalyst synthesis · homogeneous catalysis · counterion effect · kinetics

[1] A. S. K. Hashmi, M. Rudolph, *Chem. Soc. Rev.* **2008**, *37*, 1766.
[2] A. S. K. Hashmi, *Chem. Rev.* **2021**, *121*, 8309–8310.
[3] A. S. K. Hashmi, G. J. Hutchings, *Angew. Chem. Int. Ed.* **2006**, *45*, 7896–7936.
[4] R. P. Herrera, M. C. Gimeno, *Chem. Rev.* **2021**, *121*, 8311–8363.
[5] S. P. Nolan, *N-Heterocyclic Carbenes, Effective Tools for Organometallic Synthesis*, Wiley-VCH Verlag GmbH & Co. KgaA, **2014**.
[6] A. S. K. Hashmi, F. Rominger, M. Rudolph, J. Schießl, D. Zahner, T. Wurm, P. Zargaran, *Adv. Synth. Catal.* **2018**, *360*, 106–111.
[7] M. Gatto, A. Del Zotto, J. Segato, D. Zuccaccia, *Organometallics* **2018**, *37*, 4685–4691.
[8] M. Gatto, W. Baratta, P. Belanzoni, L. Belpassi, A. Del Zotto, F. Tarantelli, D. Zuccaccia, *Green Chem.* **2018**, *20*, 2125–2134.
[9] G. Ciancaleoni, L. Belpassi, D. Zuccaccia, F. Tarantelli, P. Belanzoni, *ACS Catal.* **2015**, *5*, 803–814.
[10] D. Zuccaccia, L. Belpassi, F. Tarantelli, A. Macchioni, *J. Am. Chem. Soc.* **2009**, *131*, 3170–3171.
[11] Z. Lu, T. Li, S. R. Mudshinge, B. Xu, G. B. Hammond, *Chem. Rev.* **2021**, *121*, 8452–8477.
[12] L. Biasiolo, A. Del Zotto, D. Zuccaccia, *Organometallics* **2015**, *34*, 1759–1765.
[13] M. Gatto, P. Belanzoni, L. Belpassi, L. Biasiolo, A. Del Zotto, F. Tarantelli, D. Zuccaccia, *ACS Catal.* **2016**, *6*, 7363–7376.
[14] J. Cordón, J. M. López-de-Luzuriaga, M. Monge, *Organometallics* **2016**, *35*, 732–740.
[15] M. Kumar, J. Jasinski, G. B. Hammond, B. Xu, *Chem. Eur. J.* **2014**, *20*, 3113–3119.
[16] A. Zhdanko, M. E. Maier, *ACS Catal.* **2015**, *5*, 5994–6004.
[17] C. Tubaro, M. Baron, M. Costante, M. Basato, A. Biffis, A. Gennaro, A. A. Isse, C. Graiff, G. Accorsi, *Dalton Trans.* **2013**, *42*, 10952– 10963.
[18] G. Trevisan, V. Vitali, C. Tubaro, C. Graiff, A. Marchenko, G. Koidan, A. N. Hurieva, A. Kostyuk, M. Mauceri, F. Rizzolio, G. Accorsi, A. Biffis, *Dalton Trans.* **2021**, *50*, 13554–13560.
[19] M. Baron, E. Battistel, C. Tubaro, A. Biffis, L. Armelao, M. Rancan, C. Graiff, *Organometallics* **2018**, *37*, 4213–4223.
[20] T. A. C. A. Bayrakdar, T. Scattolin, X. Ma, S. P. Nolan, *Chem. Soc. Rev.* **2020**, *49*, 7044–7100.
[21] E. Marcheggiani, C. Tubaro, A. Biffis, C. Graiff, M. Baron, *Catalysts* **2020**, *10*, 1.
[22] M. H. Larsen, K. N. Houk, A. S. K. Hashmi, *J. Am. Chem. Soc.* **2015**, *137*, 10668–10676.
[23] A. S. K. Hashmi, *Acc. Chem. Res.* **2014**, *47*, 864–876.
[24] A. Gómez-Suárez, S. P. Nolan, *Angew. Chem. Int. Ed.* **2012**, *51*, 8156–8159.
[25] J. Roithová, Š. Janková, L. Jašíková, J. Váňa, S. Hybelbauerová, *Angew. Chem.* **2012**, *124*, 8503–8507.
[26] A. Zhdanko, M. E. Maier, *Chem. Eur. J.* **2014**, *20*, 1918–1930.
[27] A. Gómez-Suárez, Y. Oonishi, A. R. Martin, S. V. C. Vummaleti, D. J. Nelson, D. B. Cordes, A. M. Z. Slawin, L. Cavallo, S. P. Nolan, A. Poater, *Chem. Eur. J.* **2016**, *22*, 1125–1132.
[28] P. de Frémont, R. Singh, E. D. Stevens, J. L. Petersen, S. P. Nolan, *Organometallics* **2007**, *26*, 1376–1385.
[29] L. Biasiolo, M. Trinchillo, P. Belanzoni, L. Belpassi, V. Busico, G. Ciancaleoni, A. D'Amora, A. Macchioni, F. Tarantelli, D. Zuccaccia, *Chem. Eur. J.* **2014**, *20*, 14594–14598.
[30] M. Baron, C. Tubaro, M. Basato, A. A. Isse, A. Gennaro, L. Cavallo, C. Graiff, A. Dolmella, L. Falivene, L. Caporaso, *Chem. Eur. J.* **2016**, *22*, 10211–10224.
[31] M. Monticelli, M. Baron, C. Tubaro, S. Bellemin-Laponnaz, C. Graiff, G. Bottaro, L. Armelao, L. Orian, *ACS Omega* **2019**, *4*, 4192–4205.
[32] A. Marchenko, G. Koidan, A. Hurieva, Y. Vlasenko, A. Kostyuk, A. Lenarda, A. Biffis, C. Tubaro, M. Baron, C. Graiff, F. Nestola, *J. Organomet. Chem.* **2017**, *829*, 71–78.
[33] M. Baron, C. Tubaro, A. Biffis, M. Basato, C. Graiff, A. Poater, L. Cavallo, N. Armaroli, G. Accorsi, *Inorg. Chem.* **2012**, *51*, 1778–1784.
[34] L. Biasiolo, L. Belpassi, G. Ciancaleoni, A. Macchioni, F. Tarantelli, D. Zuccaccia, *Polyhedron* **2015**, *92*, 52–59.
[35] L. Sian, A. Guerriero, M. Peruzzini, C. Zuccaccia, L. Gonsalvi, A. Macchioni, *Organometallics* **2020**, *39*, 941–948.
[36] C. Schmidt, L. Albrecht, S. Balasupramaniam, R. Misgeld, B. Karge, M. Brönstrup, A. Prokop, K. Baumann, S. Reichl, I. Ott, *Metallomics* **2019**, *11*, 533–545.
[37] S. K. Goetzfried, C. M. Gallati, M. Cziferszky, R. A. Talmazan, K. Wurst, K. R. Liedl, M. Podewitz, R. Gust, *Inorg. Chem.* **2020**, *59*, 15312–15323.
[38] R. Mills, *J. Phys. Chem.* **1973**, *77*, 685–688.
[39] A. Macchioni, G. Ciancaleoni, C. Zuccaccia, D. Zuccaccia, *Chem. Soc. Rev.* **2008**, *37*, 479–489.
[40] D. Zuccaccia, A. Macchioni, *Organometallics* **2005**, *24*, 3476–3486.

Manuscript received: August 2, 2023
Revised manuscript received: October 24, 2023
Accepted manuscript online: October 30, 2023
Version of record online: ■■, ■■

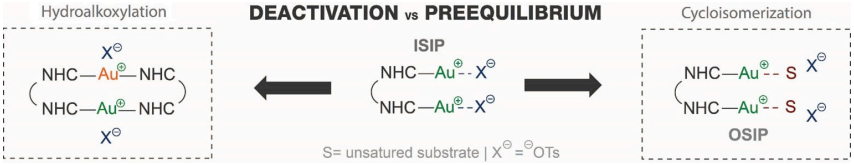

The catalytic activity of dinuclear gold(I) complexes depends on the nature of the counterion and on the linker length. Both factors influence two main important steps in hydromethoxylation of 3-hexyne and cycloisomerization of *N*-(prop-2-yn-1-yl)benzamide: deactivation and pre-equilibrium (formation of active intimate OSIP ion pairs)

F. Campagnolo, M. Bevilacqua, Dr. M. Baron, Prof. Dr. C. Tubaro, Prof. Dr. A. Biffis, Prof. Dr. D. Zuccaccia**

1 – 7

Insights on the Anion Effect in N-heterocyclic Carbene Based Dinuclear Gold(I) Catalysts